Ferdinand Hendriks

Bounce and Chaotic Motion in Impact Print Hammers

The basis of this paper is a lumped-parameter description of an impact printer actuator of the stored-energy type. All constants necessary to describe the actuator and the ribbon/paper pack are derived from measurements. The equations of motion are integrated both for single- and multiple-current pulse excitation. The numerical results show that for low repetition rates, each impact is distinct and independent, but at higher rates the impacts interact. The interaction manifests itself initially as flight-time and print-force variations: Strict periodicity of the actuator motion is lost, as shown in Poincaré plots for the actuator motion, and randomness sets in. At extremely high repetition rates, the actuator "hangs up" and the backstop no longer participates in the actuator dynamics. During settle-out the actuator motion is extremely sensitive to the timing of the current excitation. This fact can, in principle, be exploited to achieve extremely fast cycle times. However, without knowledge of the state of the actuator, as is commonly the case, this sensitivity is detrimental to print quality.

Introduction

At this time, impact printing is the most cost-effective way to obtain hard copy computer output. Because of their greater flexibility, dot matrix printers are becoming more popular than printers which use fully formed characters. The analysis presented in this paper applies to dot matrix actuators having a single moving element; this excludes dot matrix actuators with ballistic elements. In dot matrix printers of low to medium throughput (up to about 500 characters per second) the actuators are usually arranged in a cluster. The indenting elements, commonly wear-resistant wires, are arranged in one or more vertical columns. By moving these across a line, characters are formed serially, from left to right or from right to left depending on the motion of the carriage that carries the serial print head. Thanks in part to the large amount of energy delivered to the impacting element, typically one millijoule per dot, and the large forces generated, $\approx$2.3 kilograms per dot (about five pounds per dot), impact printers possess extraordinary ruggedness when compared to non-impact printers, such as ink jet and electrophotographic printers. The traditional disadvantages of impact printers, such as low throughput, low print resolution, and high power dissipation, are being offset by advances in the use of the available hardware made possible by microprocessors. Examples are print heads that do not waste time scanning areas on the paper that are to be left blank and software that allows a number of tradeoffs between speed and print quality. The ability of impact printers to produce multiple copies remains an advantage in many applications. Despite these innovations, further advances in impact print hammer technology are needed to offset their inherent disadvantages. Printer actuator mechanisms must become faster, more energy-efficient, and more versatile, preferably without giving up tolerance to variations in operating conditions (wire travel, number of forms, etc.)

The broad issues concerning throughput and characteristics of impact and non-impact printers were discussed in a recent review by Myers and Wang [1], to which the reader is referred for more information. The scope of the present paper is more limited, but it deals in greater detail with an important question that arises in impact printing: What happens to an impact printer actuator and the print quality when the frequency of actuation increases?

Various workers [1–3] in the field of impact printing have dealt with the factors that limit performance in impact actuators. It was found in general that performance is limited by inefficient design of the magnetic circuit, leading to overheating. There are also mechanical effects such as unwanted resonance that limit the operating range of actuators and print quality. These observations have shaped the manner in which actuator design is now being approached.

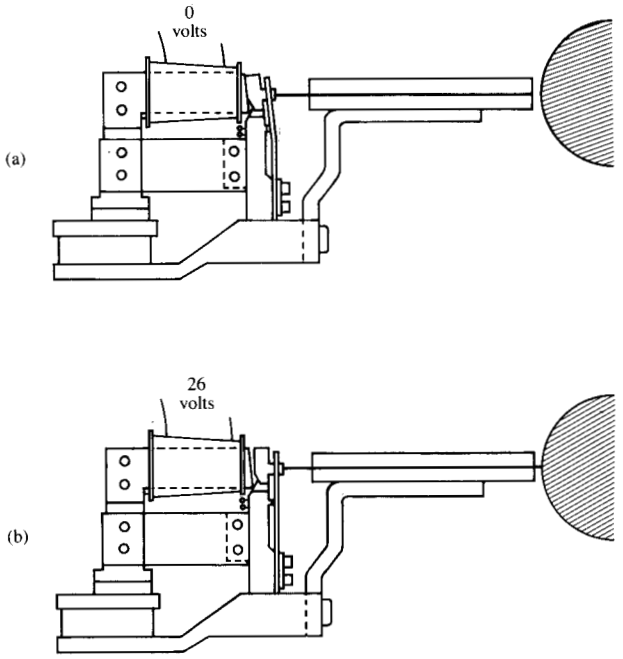

Figure 1 Impact actuator of the stored-energy type, showing the retracted print wire in the (a) normal and (b) print positions.

Largely through a careful process of design iteration, acceptable magnetic design can be arrived at, in some cases guided by finite-element solutions to the magnetic field equations, but rarely accounting for the effect of eddy currents. As far as the mechanical design is concerned, the importance of the mass and finite stiffness of print hammers of the lever type, leading to such phenomena as double impact, is widely recognized. In at least one design, "the whipping hammer" [2], flexibility is cleverly exploited to reduce the contact time of the indenter on the ribbon/paper pack in an engraved-character line printer.

From these prior studies we may conclude that the behavior of print hammers during the acceleration phase is relatively well understood, whereas what happens after the printer armature returns from the paper has been given comparatively little attention. This is not surprising, because the numerical effort and computer resources required to compute magnetic fields and structural vibrations of print hammers are vast. Hence, insight gained with these methods was typically limited to the acceleration phase of the actuator. That was adequate in low-speed line printers, but in present dot matrix applications and in fast engraved-character line printing, the actuator return and settle-out phases are equally important. Therefore, the present paper deals primarily with print hammers under repeated excitation, where the return and settle-out phases have to be taken into account.

To keep the expense of numerical computation within reasonable bounds, a lumped-parameter description of the actuator is adopted. At first sight, such a description might not seem to offer much hope for interesting results, but it becomes clear shortly that the bounce phenomenon, combined with forcing at high frequency, produces a response of great complexity and significance. Even more importantly, we contend that the simple model used here can explain many of the ills actuators experience when forced hard.

In dot matrix printing, high repetition rates, of the order of 1 kHz and faster, can only be achieved when one foregoes the luxury of waiting for complete settle-out. Re-firing of the actuator during the settle-out phase entails larger flight-time variations, but large flight-time variations, of the order of 200 microseconds (μs) peak to peak, are commonly accepted in the industry as long as the impact forces are adequate. This is in contrast with engraved-character line printers, in which there is virtually no tolerance for incomplete settle-out. The reason is that in the latter the hammer must strike a rapidly moving fully formed character on a print belt at a very precise location and time. The belt moves past a platen and its speed can, in some printers, exceed 10 m/s. Severe print quality degradation, such as clipping of the printed characters, occurs when the flight time varies more than a few tens of microseconds. In dot matrix printing, on the other hand, the relative motion between the hammer and the paper is only a fraction of a meter per second, making flight-time variations relatively harmless.

In both forms of impact printing, the consequence of bounce is always reduced print quality. In engraved-character line printers, it is misregistration and slur; in dot matrix printers, it is nonuniform print density and even missing dots. In the remainder of this paper we shall limit ourselves to a discussion of dot matrix printing, concentrating on a stored-energy actuator.

The stored-energy actuator

One of the fastest types of actuator is the stored-energy actuator, also known as a "no-work" actuator. In this type of actuator (see Fig. 1), the armature or, in some actuators, a flexing beam, is stressed by a permanent magnet. A coil is arranged in such a way that, when energized with a current of appropriate sense and magnitude, the armature is released, thus striking the ribbon and paper. The force due to the permanent magnet and the "bucking coil" and that due to the spring are shown in Fig. 2 for various current levels. When the armature is close to the backstop (position is shown by labeled vertical line in figure), the force on the armature is very sensitive to the coil current. Consequently, much less control can be exerted when the armature is released. When one compares the reflection of the spring force (dashed line in lower half of Fig. 2) with the magnetic

force at zero current, it becomes evident that the force to fire the hammer from rest depends on the *small difference* between the spring force and the net magnetic force.

The permanent magnet recaptures the armature upon returning. Meant to be short, the capturing phase still has some finite duration, during which the actuator settles out. Fast actuators invariably suffer from bounce, although it can be minimized with the use of damping materials, such as hysteretic polymers, and by eddy-current and active damping.

Mathematical model

The simplest description of a stored-energy actuator is given by Newton's law for an armature represented by a mass point. This may seem too simplistic at first, but in practice many print hammers, thanks to great care in designing a light and stiff structure, behave nearly as rigid bodies, if not as mass points. Actuators that can be described as mass points represent an ideal structure in the sense that spurious structural modes are ruled out by definition.

If we assume that the armature displacement x is positive towards the ribbon and paper and that the armature mass is denoted by m, the equation of motion is

$$F_t = m\ddot{x}, \tag{1}$$

where F_t is the sum of all forces acting on the armature and $\ddot{x}$ is the second derivative of x with respect to time (i.e., the acceleration). The initial conditions to Eq. (1) are not known *a priori*. However, the state $\mathbf{x}(0)$, a static equilibrium, can be found by an iteration on $\mathbf{x}$ such that $F_t = 0$. At rest, the armature compresses the backstop and the Hertz contact force is in equilibrium with the spring and permanent magnet forces.

The total force on the armature is further broken down as

$$F_t = F_m + F_s + F_p + F_h + F_e, \tag{2}$$

where F_m is the net magnetic force exerted by the permanent magnet and the coil, F_s is the armature spring force, F_p is the force exerted by the ribbon/paper pack on the armature, F_h is the Hertz contact force mentioned before, and F_e is the viscoelastic force at the backstop. Note that some of the individual forces may be negligible or equal to zero over part of the range of displacement. Measurements of this force at various coil current levels I show that the expression

$$F_m = F_0 - \frac{(A_m - B_m I)^2}{\sqrt{x}} \tag{3}$$

fits the data very well when F_0, A_m, and B_m are suitably chosen. The forces F_m and F_0, the maximum magnetic force, are measured (as is regrettably still customary) in pounds, x in inches, and I, the coil current, in amperes. (*Editor's note*: SI metric conversion values appear in parentheses next to these values, and as separate axes in the figures.) Figure 2 shows the magnetic force F_m at various current levels in relation to the armature spring force F_s, given by

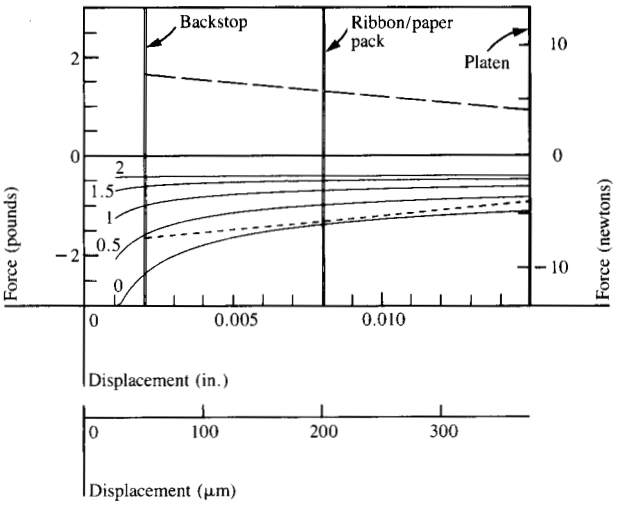

Figure 2 Solid curves show the net magnetic force F_m vs. the displacement distance at various coil currents (0, 0.5, 1, 1.5, and 2 amps). Also shown are the linear spring force F_s (——) and its reflection (---). At zero current, return of the armature from any displacement is ensured since the net force on the armature at zero current always drives the armature against the backstop. The double vertical lines indicate the relative positions of the backstop, ribbon/paper pack, and platen. Note that the position of the backstop has been arbitrarily set at 0.002 in. (51 μm).

$$F_s = B_s - \frac{B_s}{A_s}(x - b), \tag{4}$$

with constants A_s and B_s provided by experiment. The parameter b is the position of the backstop, which in this paper is arbitrarily set to 0.002 inches (51 μm).

Several authors (see for example Dauer [4]) have measured the characteristics of substrates (ribbon and single- or multi-part forms). For dot matrix printing, Wang and Hall [5] have found that

$$F_p = -(A_i E_p)\left\{H(\dot{x})\left(\frac{x - x_p}{d}\right)^{2.7} + H(-\dot{x})\left(\frac{x_{max}}{d}\right)^{-8.3}\left(\frac{x - x_p}{d}\right)^{11}\right\}, \tag{5}$$

where E_p is a constant that can be interpreted as a characteristic ribbon/paper stiffness, and A_i is the area of the indenter of the ribbon/paper pack; i.e., in a wire matrix printer it is the cross-sectional area of the wire; x_p is the position of the armature at which it just touches the ribbon/paper pack from an arbitrarily chosen origin, d is the ribbon/paper pack

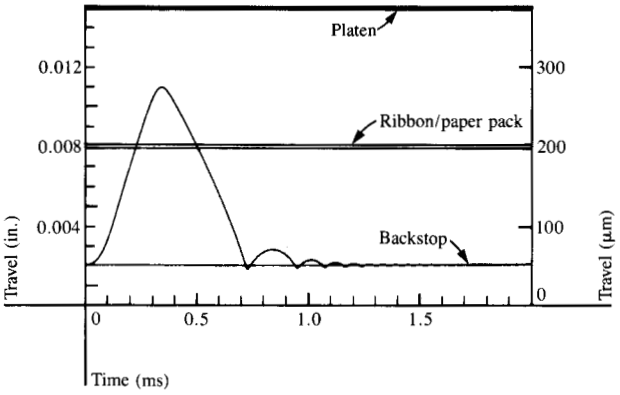

Figure 3 Hammer motion resulting from single-pulse excitation. The horizontal lines indicate the relative positions of the backstop at 0.002 in. (51 μm), the ribbon/paper pack at 0.008 in. (203 μm), and the platen at 0.015 in. (381 μm).

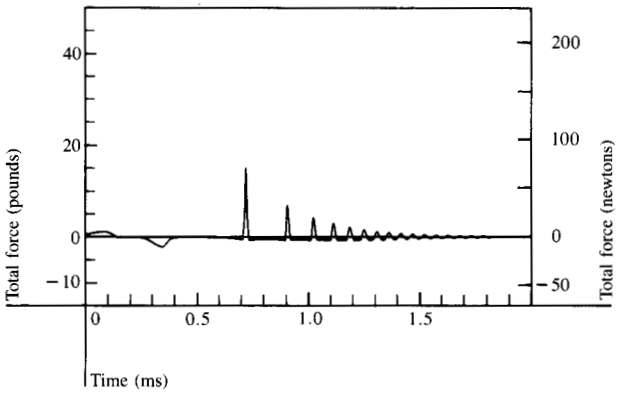

Figure 4 Total force on the armature as a function of time for single-pulse excitation.

thickness, and $\dot{x}$ is the first derivative of x with respect to time (i.e., the velocity). This expression describes the "paper force" very well as long as there is no mechanical failure of the ribbon/paper and the paper has not been indented before. Also, the subtle effects of relative humidity and plastic memory have been neglected. The function $H(\dot{x})$ is the unit step function and x_{max} is the maximum indentation of the printing substrate. Note that there can be local maxima.

Upon returning from the paper, the armature hits the backstop, whose primary purpose is to bring the armature to rest and to provide well-defined initial conditions for subsequent actuations. There are two radically different approaches to achieve rapid settle-out. The first approach relies on the hysteresis exhibited by some elastomers. Backstops made of such material undergo rather large deformation, typically of the order of 0.001 in. (25 μm), while the forces remain rather small (a few pounds). Settle-out on elastomers happens with few rebounds. Some actuators lack compliant backstops. Instead we may find backstops made of steel, often coated with chromium for wear resistance. Settle-out against this type of backstop shows many more rebounds of successively smaller amplitude. Especially when the actuator is of stored-energy type, the frequency of bounce during settle-out can be very high. Thus, while the energy dissipated per bounce may be only moderate, the fact that there are many bounces at gradually increasing frequency causes the average energy dissipation to be high. It is not always clear what the source of energy dissipation is for hard backstops. Often, the question is left unanswered and a coefficient of restitution is adopted. Several mechanisms can account for the observed dissipation. The most important ones are (a) damping due to mechanical radiation [6], (b) eddy-current damping, and (c) magnetomechanical damping [7].

During observations of the actuator being described here, the rebound speeds of the armature were significantly lower than those predicted by known coefficients of restitution observed for impacting steel bodies; see Goldsmith [8]. It became clear very quickly that cause (c) alone could not explain the observed energy loss. To account for the observed behavior, the following model was adopted. First, there is the classical Hertz contact force

$$F_h = k|b - x|^{1.5}, \tag{6}$$

where k follows from the radii of curvature and Young's moduli of the contacting bodies. Then, there is a viscoelastic force F_e given by

$$F_e = -\ell\dot{x}|b - x|^{1.5}H(b - x), \tag{7}$$

in which the constant ℓ can be viewed as a damping coefficient. Hunt and Crossley [9] arrived at a similar expression. Equation (7) allows the forces on the backstop to remain finite, while ensuring the correct change in kinetic energy after impact. Radiation damping mimics the effect of Eq. (7) in the sense that a point on a beam that undergoes a local impact leaves the impact point with diminished velocity while the total kinetic energy of the beam is conserved. Damping under those conditions can then take place remotely, such as by friction at a clamping location.

So far, the coupling between the mechanics and magnetics of the actuator has been excluded from the discussion. Strictly speaking, Faraday's law should complement the equations of motion. Most hammer-driving circuits, however, are not much affected by the reluctance changes of a stored-energy printer actuator. At most, the hammer impact is discernible on the coil current waveform as a slight cusp, if indeed the coil current has not been interrupted at that point.

Numerical integration and graphics

Integration of the equations of motion was performed initially with the implicit trapezoidal rule, which features excellent stability against the difficulties imposed by the impact of the armature on the backstop. The widely used fourth-order Runge-Kutta algorithm was also applied, giving higher accuracy but less numerical stability. Typical step sizes for the integration were ten microseconds when the armature was not in contact with the backstop, and one microsecond when the armature was in contact with the backstop. During the final stages of the settle-out phase the step size could safely be increased to twenty microseconds to speed up the calculations. The computer program used to analyze the behavior of the print hammer actuator is written in APL. This allows interactive specification of important parameters such as platen distance, forms thickness, current waveform, and hammer firing rate.

The computationally intensive parts of the program are written in PL/I and compiled. The object code is executed on an IBM 3081 from the APL environment via the IDAMS auxiliary processor, creating the impression to the user that the APL environment is maintained. A convenient way to interact with the program is the IBM 3277 with a graphics attachment, driving a Tektronix 618 storage tube. Thus equipped, the motion of the print hammer and various derived variables are available in pictorial form in seconds. Graphics support is provided by the RGRAFGA graphics workspace.

Single-shot hammer response

When the stored-energy hammer is excited with a single current pulse, the displacement response is as shown in Fig. 3. The hammer indents the ribbon/paper pack just once, as intended. The amplitude during the settle-out phase is small compared to the maximum hammer excursion, creating the impression that the hammer is largely settled out and ready for another firing. However, the energy of the hammer due to the field of the permanent magnet, as well as the total force on the armature, fluctuates significantly; see Fig. 4. By far the largest forces encountered by the armature are those caused by the backstop. In fact, the useful life of the actuator is, to a large extent, determined by impact wear of the armature/backstop interface. A force-displacement diagram of the actuator cycle is shown in Fig. 5, which shows the hysteresis loops in the ribbon/paper pack and in the backstop. During settle-out, the hysteresis loops become gradually smaller. Clockwise loops indicate energy input, counterclockwise loops indicate energy loss. The large impulsive forces at the backstop cause near-discontinuities in the hammer velocity. This sets the stage for great sensitivity of the hammer response to past firings.

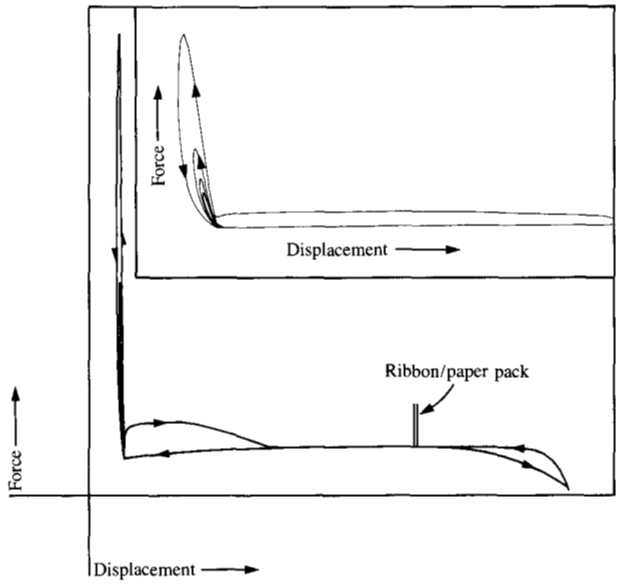

Figure 5 Force-displacement diagram. The insert to the figure shows the tightly nested hysteresis loops that correspond to settle-out.

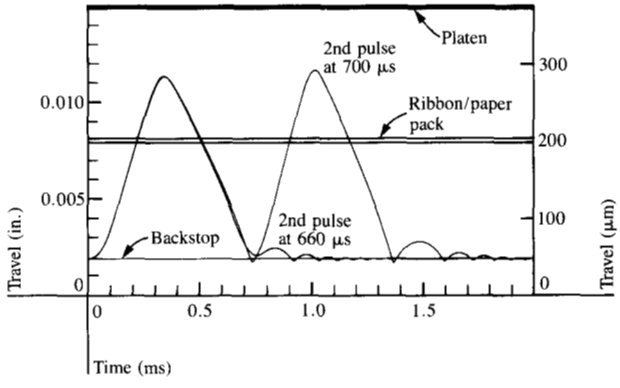

Figure 6 Hammer response to two pulses, illustrating the sensitivity to timing of the second pulse. Horizontal lines indicate the relative positions of the platen, ribbon/paper pack, and backstop.

Hammer response to multiple excitation

When there is multiple-hammer excitation there is opportunity for the hammer to react to past hammer firings. A striking example is presented in Fig. 6. In this two-pulse example, a 40-microsecond difference in firing time (660 vs. 700 μs) causes the response to the second waveform to change from braked or quenched response to a complete hammer excursion. The pulse with the longest delay (700 microseconds) causes a 10% stronger impact on the paper, because the armature has a larger excursion into the ribbon/paper pack. Instead of braking the motion, the firing at 700 μs aids the motion, thus making full use of the rebound

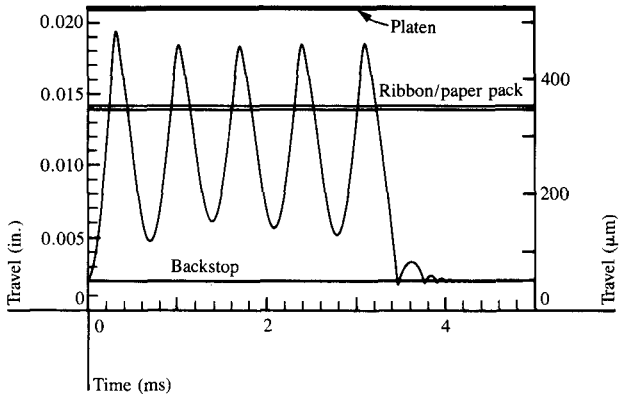

Figure 7 An example of "buzz-printing." The armature stays clear of the backstop within a print burst. Relative positions of the backstop, ribbon/paper pack, and platen are shown as horizontal lines.

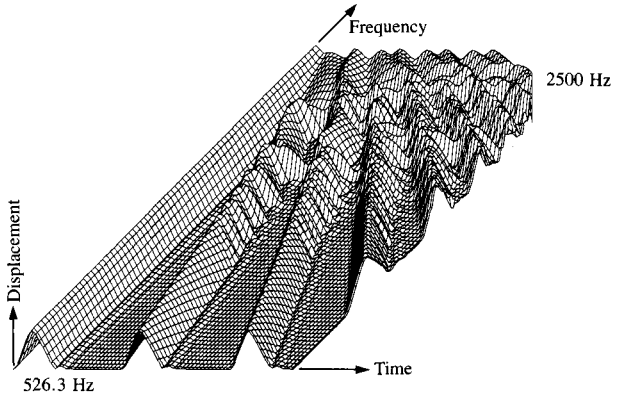

Figure 8 Hammer displacement as a function of time and forcing frequency. The hammer is excited by a nine-pulse burst.

kinetic energy. As a consequence, the hammer flight time is reduced compared to that of the first firing. Catching the hammer "on the rise" has been associated with the term "resonant printing" [10]. Still another mode of operation is possible. Instead of allowing the armature to return fully to the backstop, current pulses can be issued that are synchronized with the return of the armature from the paper. Figure 7 shows the result, sometimes known as "buzz-printing" [3]. The latter mode of operation tends to produce weak impacts on the paper. It is also quite sensitive to proper timing of the current pulse train, and to variations in the ribbon/paper pack.

Let us further explore interactions between firings to see how they depend on hammer firing frequency. To do this,

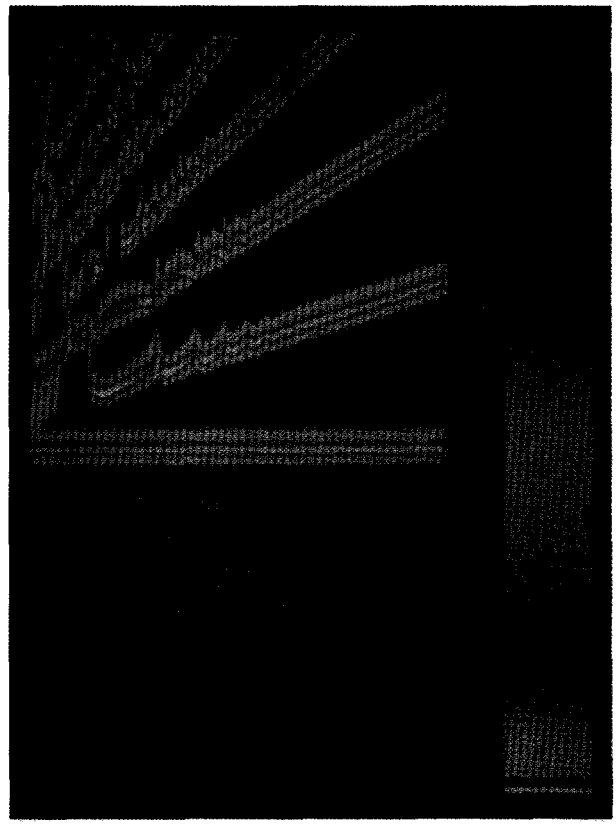

Figure 9 Frequency-time plot for nine-pulse excitation, showing the domain of erratic hammer response. Colors correspond to amplitudes of the hammer motion.

displacement vs. time plots at gradually increasing current excitation frequency are laminated together to form a three-dimensional surface; see Fig. 8. The same data, now presented as a color-enhanced picture, are shown in Fig. 9. The maximum hammer displacement at low frequency is 0.0112 in. (284 μm). Upon casual inspection, the figure shows regions, both at low and at very high frequency, in which the hammer response varies slowly with frequency. At high frequencies, the armature fails to return to the backstop and is no longer subjected to the sudden reversals of velocity. The actuator behaves as in the buzz-printing mode mentioned earlier, although the individual impacts on the paper are not distinct and forceful enough to be used for printing. At low frequency, there is enough time for settle-out to cause the energy of each impact to dissipate before it can affect the next cycle. Between these two extremes lies a region in time-frequency space in which the response is chaotic. Subsequent hammer excursions interact strongly and are extremely dependent on the frequency. If we look at the second firing in Fig. 9 at low frequency and keep our attention fixed on it, we can gradually track the second firing at increasing frequency. We observe that the second firing starts to waver in the direction of the time axis, indicating flight-time variations due to incomplete settle-out

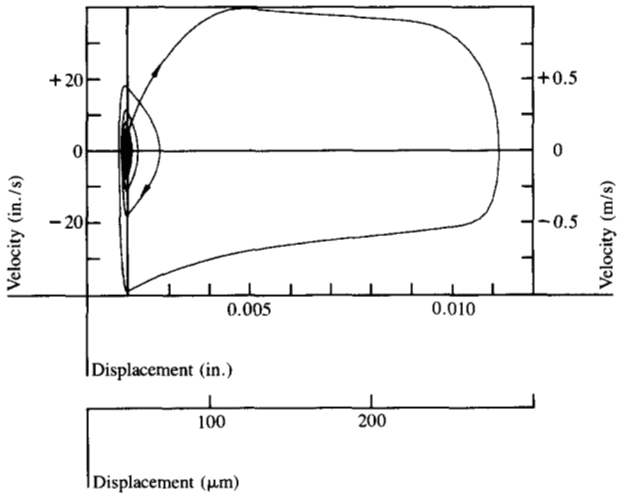

Figure 10 Actuator phase plane; arrows indicate increasing time.

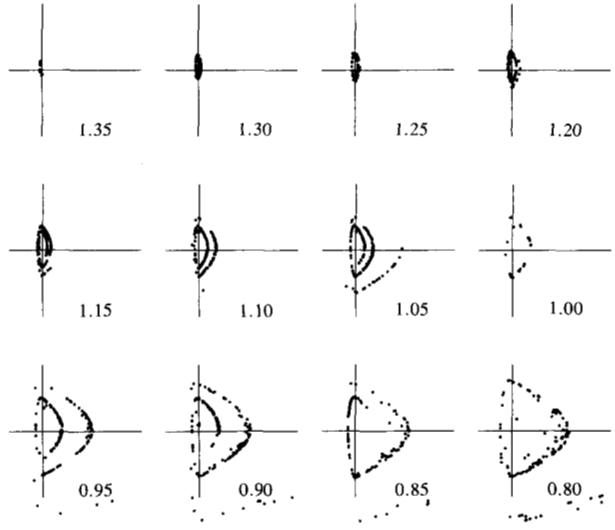

Figure 11 Sequence of Poincaré plots for the stored-energy actuator at gradually increasing rates of actuation. The numbers in the individual plots indicate the time (in ms) at which the actuator is re-fired (strobe times). All of the plots show strange attractors, except at a strobe time of 1.35 ms, where a double cycle occurs, and at strobe times of 1.30, 1.25, and 1.00 ms, where the motion is periodic at the frequency of forcing. Note the vertical lines which define the position of the backstop [arbitrarily set at 0.002 in. (51 μm)]. The abscissa extends from 0.0015 to 0.0035 in. (38 to 89 μm) and the ordinate from −25 to +25 in./s (−0.64 to +0.64 m/s). There are 200 phase points in each plot.

of the first firing. We observe also that the second firing disappears almost completely, corresponding to the second firing at 660 μs in Fig. 6. This state of affairs would lead to a missing dot on the paper.

Poincaré plots

Repeated application of current drive pulses to the actuator can be considered an iterated map in the phase plane of the actuator motion. Figure 10 shows the phase plane for a single pulse, including settle-out. If we magnify the region around the origin and study the state $(x, \dot{x})$ of the system at a specific phase of the excitation, as if with a stroboscope, we find that for low excitation frequencies the phase points converge to a single point. The response to periodic forcing is periodic with the same period. As the forcing frequency is increased, the phase points are randomly perturbed and wander in a seemingly irregular manner. They stay within a small but slowly increasing radius of the origin. The system did not undergo a series of transitions of period doubling, but double and triple cycles were observed as isolated cases among chaotic solutions. Referring to Fig. 9, this means that in the area where the response appears randomly distributed, solutions exist that are periodic at subharmonic frequencies. Figure 11 shows Poincaré plots (abscissa = displacement, ordinate = time) for the motion at gradually increasing forcing frequencies (decreasing strobe times from 1.35 to 0.80 ms) for Figs. 11(a) through (l), respectively. Note that there are 200 phase points in each plot. It is remarkable that, despite the chaotic nature of the phase points—in general, two successive phase points do not lie close to one another—the points do tend to fall on the phase trajectory of the single-pulse phase plane. It is tempting to conclude that this is the strange attractor of the actuator Eq. (1). There are, in fact, some similarities between the actuator equation and Duffing's equation, which has a strange attractor that has been studied extensively [11]. The paper and backstop can be viewed as a hard spring, analogous to the cubic term in Duffing's equation. The actuator has very localized damping as opposed to the distributed damping in Duffing's equation.

Discussion

By using a model of extreme simplicity, it was shown that several shortcomings of present impact printer actuators, such as print-force variations and flight-time variations, can be caused *only* by imperfect settle-out. The way in which the performance of a stored-energy actuator degrades with increasing frequency of forcing was demonstrated in a single compact plot. It is hoped that similar plots, derived from experimental displacement plots, will become available in the future. The results of the simulation presented here suggest very strongly that present actuators must change in two ways if significant speed increases are to be realized: 1) passive damping methods should be improved, probably requiring a breakthrough in materials, and 2) driving current waveforms ought to respond to the phase of the hammer motion and the pattern to be printed. The latter will require more expensive and possibly less reliable hammer drivers, as well as some additional digital signal processing. These

measures should result in higher average hammer efficiencies. For example, in a typical print burst of dots, more energy might have to be expended in the first dot, but subsequent dots would be printed by keeping the actuator moving as in a parametric oscillator (swing). In the limit, the only energy to be expended should be the energy absorbed by the ribbon/paper pack, about one-half of a millijoule per dot.

Acknowledgments

I am grateful to E. Helinski for sharing his force/displacement data for stored-energy actuators with me. Several discussions with S. Hall, H.-C. Wang, C. Abul-Haj, and W. Liniger have contributed to the results of this report. Finally, I am indebted to E. Farrell, whose APL workspace IMAGE3D has contributed much to making the results of this study easier to communicate.

References and notes

1. R. A. Myers and H. C. Wang, "Les Imprimantes d'Ordinateurs," *La Récherche* **12,** 698–708 (1981).
2. H. C. Lee, D. H. Rickenbach, and J. L. Zable, "Electromagnetic Print Hammer," U.S. Patent 4,269,117 (1981).
3. E. Helinski, "Technique for Operating a Moving Coil Print Hammer," *IBM Tech. Disclosure Bull.* **22,** 8B, 3672 (1980). (The term "buzz printing" seems to have been coined by A. Fleek, IBM System Products Division, Raleigh, NC.)
4. F. Dauer, *On the Mechanics and Design of Impact Printing Devices*, University Microfilms International, Ann Arbor, MI, 1981.
5. H. C. Wang and S. A. Hall, "Paper-Function Model for Wire Matrix Printing," *Proceedings of the Society for Information Display*, **24** (1983, in press).
6. M. Takamura, "Contact Chatter of Switching Relays," *Proceedings of the NARM Ninth Annual Relay Symposium*, Stillwater, OK, 1961, pp. 61–64.
7. W. T. Cooke, "The Variation of the Internal Friction and Elastic Constants with Magnetization in Iron. Part I," *Phys. Rev.* **50,** 1158–1164 (1936).
8. W. Goldsmith, *Impact*, Edward Arnold, London, 1960.
9. K. H. Hunt and F. R. E. Crossley, "Coefficient of Restitution Interpreted as Damping in Vibroimpact," *Trans. ASME, J. Appl. Mech., Series E* **42,** 440–445 (June 1975).
10. Robert W. Kulterman, IBM Communication Products Division Laboratory, 11400 Burnet Rd., Austin, TX 78758, and Shawn Hall, IBM Thomas J. Watson Research Center, P.O. Box 218, Yorktown Heights, NY 10598; private communication.
11. M. J. Feigenbaum, "Qualitative Universality for a Class of Nonlinear Transformations," *J. Statist. Phys.* **19,** 25–52 (1979).

Received November 18, 1982

Ferdinand Hendriks *IBM General Products Division, 5600 Cottle Road, San Jose, California 95193.*
 In 1968 Dr. Hendriks obtained an M.S. in theoretical aerodynamics at the Delft Institute of Technology, The Netherlands. He was the recipient of a NASA International Fellowship from 1968 to 1970, studying at the University of California, Los Angeles; he obtained a Ph.D. in engineering science in 1973. Also in 1973, he joined IBM in the Research Division at Yorktown Heights, New York, where he investigated aerodynamic aspects of ink jet printing. For the past two years he has been manager of printer mechanics, dealing with the mechanics of impact printing. At present, Dr. Hendriks is on temporary assignment with the General Products Division in San Jose.